



PAPER • OPEN ACCESS

Synthesis and characterization of novel silver nanoparticles using *Chamaemelum nobile* extract for antibacterial application

To cite this article: Hoda Erjaee *et al* 2017 *Adv. Nat. Sci: Nanosci. Nanotechnol.* **8** 025004

View the [article online](#) for updates and enhancements.

You may also like

- [Assessing compatibility of direct detection data: halo-independent global likelihood analyses](#)
Graciela B. Gelmini, Ji-Haeng Huh and Samuel J. Witte
- [The influence of particle size and multi-walled carbon nanotube on physical properties of mineral trioxide aggregate](#)
Mohammad Reza Sanaee, Habib Danesh Manesh, Kamal Janghorban et al.
- [Study on HPLC Fingerprint of Dendrobium Nobile Lindl. Flower Based on Chemometrics](#)
Ke Zhong and Tingting Yang

Synthesis and characterization of novel silver nanoparticles using *Chamaemelum nobile* extract for antibacterial application

Hoda Erjaee¹, Hamid Rajaian¹ and Saeed Nazifi²

¹ Department of Pharmacology, School of Veterinary Medicine, Shiraz University, Shiraz, Iran

² Department of Clinical Studies, School of Veterinary Medicine, Shiraz University, Shiraz, Iran

E-mail: hodaerjaee@shirazu.ac.ir

Received 9 November 2016

Accepted for publication 13 March 2017

Published 5 May 2017



Abstract

The present study reports green synthesis of silver nanoparticles (AgNPs) at room temperature using aqueous *Chamaemelum nobile* extract for the first time. The effect of silver nitrate concentration, quantity of the plant extract and the reaction time on particle size was optimized and studied by UV–Vis spectroscopy and dynamic light scattering. The appearance of brownish color with λ_{\max} of 422 nm confirmed the formation of AgNPs. Synthesized nanoparticles were further characterized by Fourier transform infrared spectroscopy, x-ray diffraction and transmission electron microscopy. In addition, antimicrobial activity of the AgNPs against *Escherichia coli*, *Salmonella typhimurium*, *Staphylococcus aureus* and *Bacillus subtilis* was evaluated based on the inhibition zone using the disc-diffusion assay and measurement of minimal inhibition concentration and minimal bactericidal concentration by standard microdilution method. In conclusion, synthesis of nanoparticle with aqueous *Chamaemelum nobile* extract is simple, rapid, environmentally benign and inexpensive. Moreover, these synthesized nanoparticles exhibit significant antibacterial activity.

Keywords: silver nanoparticles, green synthesis, *chamaemelum nobile*, antibacterial activity

Classification numbers: 2.03, 4.02, 5.02

1. Introduction

The field of nanotechnology is one of the emerging areas of research in modern materials science, especially in biotechnology [1]. Nowadays, noble metal nanoparticles are being used in a broad range of application in the fields of biology, medicine, physics, chemistry and material science [2, 3]. Among nanostructured noble metals the most important commercialized nanoparticles are silver nanoparticles (AgNPs). AgNPs have attracted considerable attention for their application in molecular imaging [4], drug delivery [5], photonics [6, 7], micro-electronics [8], biomedicine [9, 10] and biosensors [11].

Different physical and chemical techniques have been adapted throughout the world to develop AgNPs. In recent years, attention has been focused on the use of environmentally benign materials like plant extracts, bacteria and fungi for the synthesis of nanoparticle and green synthesis of metal nanoparticles has received considerable attention because of its numerous benefits over other chemical and physical methods [12, 13]. Green synthesis of nanoparticles is a simple and reliable method which creates nanoparticle with good stability and appropriate dimensions. Plant-mediated nanoparticles synthesis is preferred because it is possible to produce large scale nanoparticles with a negligible cost; it is environmental friendly and, at the same time, safe for human therapeutic use [14]. Although synthesis of AgNPs by plant extracts has already been reported with different plants such as *Terminalia cuneata* [15], *Erythrina indica lam* [16], *Calotropis gigantea L.* [17], *Pistacia atlantica* [18], *Cocos nucifera* [19], *Alternanthera*



Original content from this work may be used under the terms of the [Creative Commons Attribution 3.0 licence](https://creativecommons.org/licenses/by/3.0/). Any further distribution of this work must maintain attribution to the author(s) and the title of the work, journal citation and DOI.

Table 1. The effect of different parameters on particle size of AgNPs.

Trial number	Quantity of extract (ml)	AgNO ₃ concentration (mM)	Reaction time (h)	^a Size of AgNP	^b Peak of Absorbance
1	0.5	0.5	8	123.1	460
2	0.5	1	8	264.3	476
3	0.5	0.5	16	92.3	458
4	0.5	0.5	24	75	442
5	0.5	1	16	195.2	472
6	0.5	1	24	179.5	470
7	1	0.5	8	63.3	438
8	1	0.5	16	52	428
9	1	0.5	24	47.3	422
10	1	1	8	174	468
11	1	1	16	106.1	456
12	1	1	24	75	452

^a Average particle size measured by DLS.

^b Peak of absorbance measured by UV–Vis.

dentate [20], *Croton sparsiflorus morong* [21], *Tribulus terrestris* [22], *Desmodium gangeticum* [23] and *Prosopis farcta* [24] there is still a lot of attention paid to this field because of the diversity and the high potential of plants in producing nanoparticles with different shapes [18].

In the last three decades, there are many new antibiotics that have been produced by pharmacological industries. However, the resistance to these drugs has also increased in microorganisms. The problem of microbial resistance is growing and the outlook for the use of antimicrobial drugs in the future is still uncertain [25, 26]. Due to the increasing bacterial resistance to classic antibiotics, the development and modification of novel antimicrobial agents (e.g. natural and inorganic based antimicrobial substances) are necessary [27]. In the recent years, studies on AgNPs have developed because of their inhibitory effect on bacteria [28, 29]. Antimicrobial properties of AgNPs triggered the use of these nanoparticles in different fields of medicine, various industries, animal husbandry, packaging, cosmetics, health and military [30, 31]. Therefore, development of new AgNPs by green synthesis with active antimicrobial effect is favorable. Herein, the principal objective of this study was to achieve a novel approach for biosynthesis of AgNPs as a green chemistry method using aqueous extract of *Chamaemelum nobile* (Roman chamomile) at room temperature. Characterization of the synthesized nanoparticles was evaluated using UV–visible spectroscopy, Fourier transform infrared spectroscopy (FTIR), x-ray diffraction (XRD), transmission electron microscope (TEM) and dynamic light scattering (DLS). Furthermore, antibacterial activity of synthesized AgNPs was assessed against *Escherichia coli*, *Salmonella typhimurium*, *Staphylococcus aureus* and *Bacillus subtilis*.

2. Materials and methods

2.1. Preparation of the plant extract

Chamaemelum nobile (*C. nobile*) was obtained from Shiraz (Fars, Southern Iran). To prepare *C. nobile* aqueous extract, 5.0g of dry plant powder was crushed into 50ml of sterile

distilled water and placed in orbital shaker for 6h then the extract was filtered through whatman no.1 filter paper. The clearly filtered, light yellow extract was stored in refrigerator at 4 °C. The extract was used as reducing agent as well as stabilizing agent for producing AgNPs.

2.2. Biosynthesis of AgNPs

In order to prepare AgNPs, 5 ml of plant extract was added to 95 ml (1 mM) aqueous solution of AgNO₃ and it was incubated at room temperature. The reduction of metal ions was initially confirmed by visual inspection of color change from light brown to dark brown then by spectrophotometric absorption at 200–800nm. Various reaction parameters including quantity of plant extract, concentration of silver nitrate solution and reaction time were optimized to enhance the yield of nanoparticle at room temperature (24 °C). Spectrophotometric absorption and DLS measurements were recorded for each of the trials during the reaction time (table 1).

To remove un-reacted extract from the final solution, the reaction medium containing AgNPs was centrifuged at 10000rpm for 15 min. The obtained precipitation was freeze-dried and used for further studies.

2.3. Characterization of nanoparticles

As mentioned above, the formation of AgNPs were monitored by UV–vis absorbance. Absorbance for synthesized AgNPs was taken in the range of 200 to 800 nm using HACH-DR5000 spectrophotometer. In order to estimate the average size of nanoparticles a Microtrac Nanotracs wave particle size analyzer (Microtrac, USA) was used. TEM measurements were taken on TEM instrument (Philips CM-10 electron microscope) operated at an accelerating voltage at 100keV. Samples were prepared by drop coating of colloidal solution into formvar/carbon coated TEM grids. To identify the functional groups of synthesized nanoparticles FTIR (Perkin Elmer) spectroscopy was performed. For XRD analysis, freeze-dried nanoparticles were coated on XRD grid and the spectra were recorded using XRD instrument operating at 40kV and a current of 40 mA

with Cu-K α 1 radiation. The instrument was operated over the 2θ range of 30–80° (Phillips, USA) [32].

2.4. Antimicrobial assay

2.4.1. Bacterial strains. The antibacterial effect of AgNPs were evaluated against *E. coli* ATCC 35218, *S. typhimurium* ATCC 14028, *S. aureus* ATCC 6538 and *Bacillus subtilis* ATCC 1010649 following the guidelines of National Committee for Clinical Laboratory Standards (NCCLS 2000). Aqueous plant extract and aqueous solution of AgNO₃ were considered as comparative controls.

2.4.2. Microdilution assay. Minimal inhibition concentration (MIC) values of AgNPs and controls were determined based on a microwell dilution method using 96-well sterile microtiter plate [33]. Furthermore, AgNPs, aqueous plant extract and aqueous solution of AgNO₃ were serially diluted in Tryptic soy broth (TSA, Merck, Germany) at concentrations of 1000 $\mu\text{g ml}^{-1}$, 500 $\mu\text{g ml}^{-1}$, 250 $\mu\text{g ml}^{-1}$, 125 $\mu\text{g ml}^{-1}$, 62.5 $\mu\text{g ml}^{-1}$, 31.2 $\mu\text{g ml}^{-1}$, 15.6 $\mu\text{g ml}^{-1}$, 7.8 $\mu\text{g ml}^{-1}$, 3.9 $\mu\text{g ml}^{-1}$, 1.9 $\mu\text{g ml}^{-1}$, 0.9 $\mu\text{g ml}^{-1}$ and 0.4 $\mu\text{g ml}^{-1}$ in a final volume of 100 μl . From the bacterial suspension containing 10⁶ CFU ml⁻¹ bacteria, 10 μl was inoculated in wells. Moreover, the bacterial suspension (without any drug) was added to three wells and served as growth control. A multi detection microplate reader (BioTek's PowerWave XS2, USA) at 600nm was used to measure optical densities in 24 h at 37 °C and the optical density (OD) for each well was recorded every 2 h spontaneously. The MIC was defined as the lowest concentration of the compounds to inhibit the growth of microorganisms. Minimal bactericidal concentration (MBC) was determined by plotting 5 μl samples from clear wells into nutrient agar plates. The MBC was the concentration at which there was no microbial growth. All experiments were performed in triplicate and results were reported in terms of mean \pm SD.

2.4.3. Disc-diffusion assay. The antimicrobial activity of biosynthesized Ag-NPs was also determined by disc diffusion method [35]. Afterward, 100 μl of the suspension containing 10⁶ CFU ml⁻¹ of the test microorganisms were swabbed uniformly on nutrient agar. The discs with 6 mm diameter were impregnated with 30 μl of AgNPs at the concentration of 39 $\mu\text{g ml}^{-1}$ for *E. coli* and *S. typhimurium*, 156.2 $\mu\text{g ml}^{-1}$ for *S. aureus* and 78 $\mu\text{g ml}^{-1}$ for *B. subtilis* (the concentrations were quintuple the MIC value). Quintuple MIC values for aqueous solution of AgNO₃ was also used as the final concentration for discs that served as negative control. In addition, tetracycline (30 $\mu\text{g/disc}$) was used for comparison. The inoculated plates were incubated at 37 °C for 24h and inhibition zones were measured in terms of the diameter (in millimeters) and compared with *C. nobile* extract, aqueous solution of AgNO₃ and tetracycline. Each assay in the experiment was performed in triplicate.



Figure 1. Synthesis of AgNPs by *C. nobile* with brown color change.

3. Results and discussion

3.1. UV-Vis spectroscopic study

As shown in figure 1, the appearance of brownish color in the reaction mixture indicates the formation of AgNPs. The change in color of the solution was due to the surface plasmon resonance (SPR) and reduction of silver ions by aqueous extract of *C. nobile*. Furthermore, the UV-Vis absorption spectrum of AgNPs in the range of 200–800 nm at the optimum condition revealed a peak at 414 nm in 2 h and 422 nm in 24 h (figure 2). This strong SPR peak confirms the formation of AgNPs. The color of the solution started to change within 20 min by the addition of aqueous plant extract and after 24 h of incubation there was no significant change, neither in color nor in the SPR peak. Moreover, AgNO₃ solution which was used as control showed no color change.

3.2. Optimization of different parameters

For the synthesis of AgNPs at room temperature, different parameters were optimized including quantity of plant extract, concentration of silver nitrate and reaction time. The different parameters and their average sizes measured by DLS are shown in table 1. Researches have reported that changes in the composition of the reaction mixture will control the properties of nanoparticles [35]. In this case, different amount of extract from various plants has been used to obtain the best morphology and size of nanoparticles. In the present study, increasing the amount of plant led to an increase in peak absorbance in UV/Vis spectrum. In addition, larger quantities of extract reduced the particle size. This finding is in agreement with the researches done by Ibrahim [35], Iravani and Zolfaghari [30].

Moreover, increasing the AgNO₃ concentration in the reaction mixture from 0.5 to 1 mmol l⁻¹ led to AgNPs with larger size. Meanwhile, enhancement of the reaction time from 8 to 24 h caused reduction in the size of AgNPs. These results are in agreement with the earlier investigations conducted by Gavade et al [36], Krishnaraj et al [37] and Pourmortazavi et al [38]. Therefore, to produce the smallest size of AgNPs by *C. nobile* aqueous extract at room temperature, the optimum condition is as following: 0.5 mmol l⁻¹ silver ion concentration, reaction time of 24 h, and 1 ml plant extract (trial number 9, table 1).

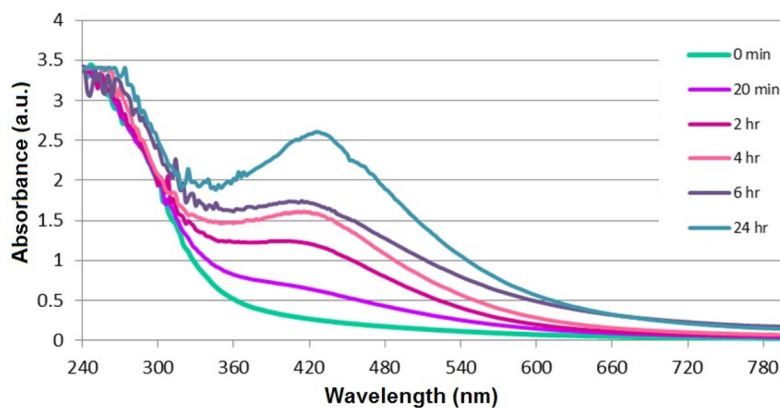


Figure 2. UV-Vis absorption spectra of AgNPs at optimum condition.

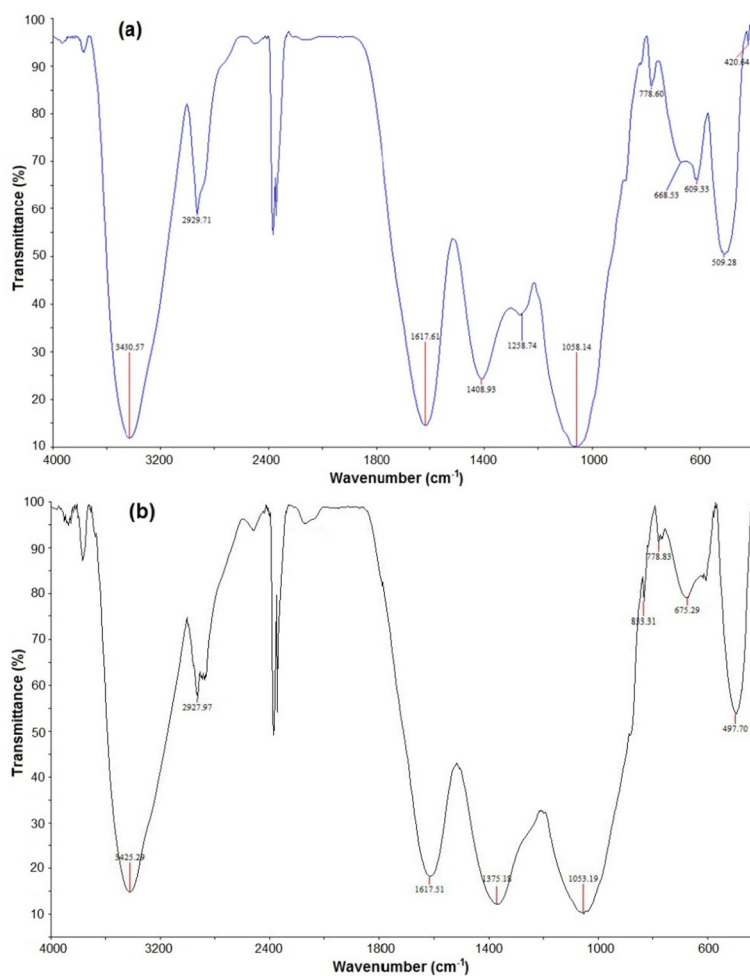


Figure 3. FTIR spectra of *C. nobile* aqueous extract (a) and AgNPs (b).

3.3. FTIR spectroscopy analysis

FTIR measurements were carried out to identify various functional groups in *C. nobile* extract which are responsible for reducing and stabilizing the synthesized AgNPs. The FTIR spectra of control plant extract and synthesized Ag-NPs are shown in figures 3(a) and (b), respectively. FTIR analysis showed strong bands at 3430 cm⁻¹, 2929 cm⁻¹, 1617 cm⁻¹, 1408 cm⁻¹, 1258 cm⁻¹, 1058 cm⁻¹ and 668 cm⁻¹ for control extract, and 3425 cm⁻¹, 2927 cm⁻¹, 1617 cm⁻¹,

1375 cm⁻¹, 1053 cm⁻¹ and 675 cm⁻¹ for synthesized AgNPs. A broad peak at 3430 cm⁻¹ (*C. nobile* extract) and 3425 cm⁻¹ (AgNPs) is characteristic of the O-H stretch of hydrogen bonded phenolic and flavonoid group present in the phytoconstituents. The peaks observed at 2929 cm⁻¹ can be assigned to the C-H group which was shifted to the lower frequency (2927 cm⁻¹) in AgNPs when compare to the extract. The peak observed at 1617 cm⁻¹ is assigned to bounded amine groups (-NH) of leaf extract. The band at 1408 cm⁻¹ and 1258 cm⁻¹ denoted the phenolic groups of tannin existing in

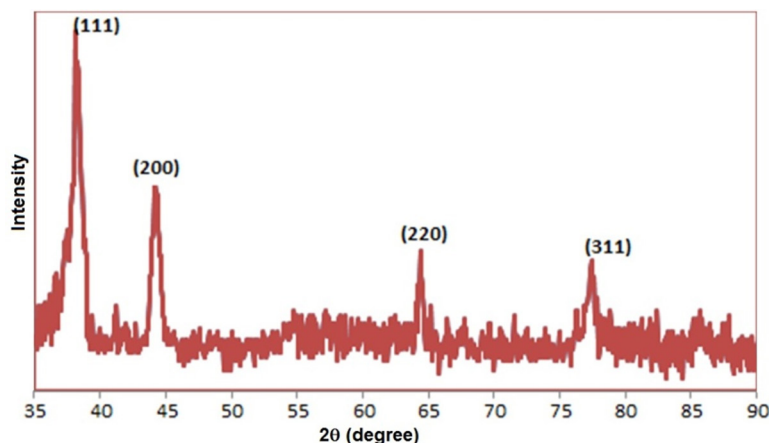


Figure 4. X-ray diffraction profile of biosynthesized AgNPs.

C. nobile extract. As it is shown in figure 3(b), these peaks are missing in the FTIR spectra of the AgNPs indicating that the O–H groups were one of the groups responsible for synthesis of AgNPs. Furthermore, the IR spectra of AgNPs showed an absorption band at 1375 cm^{-1} , corresponding to the NO_3 stretching which is due to the residue of silver nitrate. The peak at 1058 cm^{-1} was attributed to the C–O group which is shifted to 1053 cm^{-1} after the reduction of silver. The band at the peak observed at 1617 and 675 cm^{-1} is assigned to bounded amine groups (–NH) of leaf extract. 675 cm^{-1} peak also shifted to 668 cm^{-1} after the reduction of silver. It is well known that biological components interact with metal salts and mediate reduction process with these functional groups [39]. Comparison of the FTIR spectra of AgNPs with *C. nobile* aqueous extract revealed the presence of functional groups such as amines, carboxylic acids, aldehydes and alcohols which are responsible for reducing and capping the silver ions [40].

3.4. XRD analysis

The XRD spectrum was recorded to confirm the crystalline structure of synthesized AgNP (figure 4). The diffraction peaks were observed at 38.1° , 44.2° , 64.4° and 77.4° in the 2θ range. The peaks can be indexed to the (1 1 1), (2 0 0) and (3 1 1) reflections of face centered cubic structure of metallic silver which suitably matched the standard diffraction data with those reported for silver by joint committee on powder diffraction standards (JCPDS) file no: 040783. The average estimated crystallite size of the synthesized AgNPs at optimum condition was in the range of 24 nm. These results were consistent with the sizes of AgNPs obtained from TEM analysis.

3.5. TEM analysis

To characterize the shape, surface morphology and size of synthesized AgNPs, TEM was used. TEM micrographs recorded from the drop coated TEM grid of the synthesized nanoparticles at optimum condition showed spherical shape AgNPs with the average size of $24.2 \pm 3.1\text{ nm}$ (figure 5). These outcomes were consistent with the sizes of AgNPs obtained from the XRD.

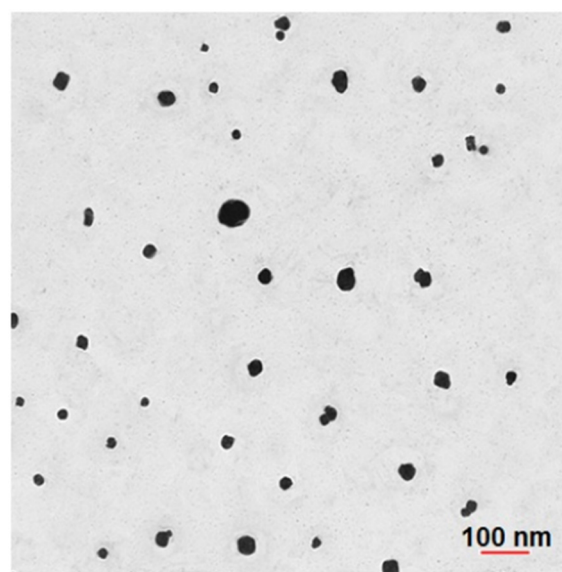


Figure 5. TEM images of synthesized AgNPs.

3.6. DLS analysis

To analyze the particle size distribution in different trials DLS was used (Microtrac, USA). Particle size measurement was done for all trials in order to choose the primary optimum size of nanoparticles (table 1). Based on the results, the mean size of AgNPs at optimum condition was recorded 47.3 nm and the range of nanoparticles was from 39 to 78.5 nm (figure 6). As expected, the DLS measured size is slightly larger than the TEM size. As it has been mentioned previously, TEM sizes were similar to XRD measurements, while the DLS sizes were significantly larger than both (table 1). The differences possibly reflect the fact that TEM only measures a number based size distribution of the physical size and does not include any capping agent, while DLS measures the hydrodynamic diameter, which is the diameter of the particle, plus ions or molecules that are attached to the surface and moves with the AgNPs in solution [41]. These ions or other associated molecules make the particle appear larger to the instrument in comparison to TEM. Hence, the hydrodynamic diameter is always greater than the size estimated by TEM [42]. Nevertheless, many

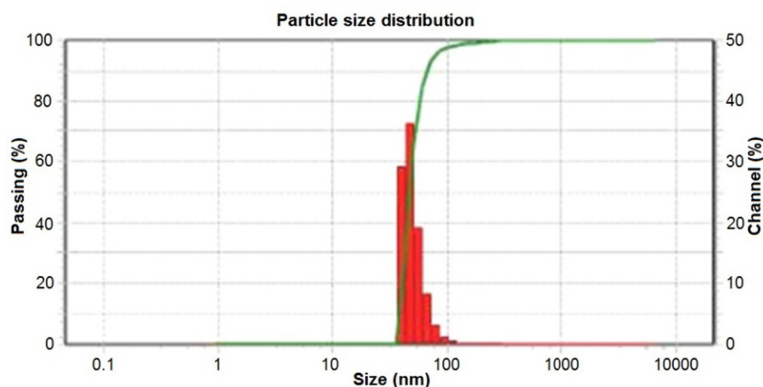


Figure 6. DLS pattern of biosynthesized AgNPs.

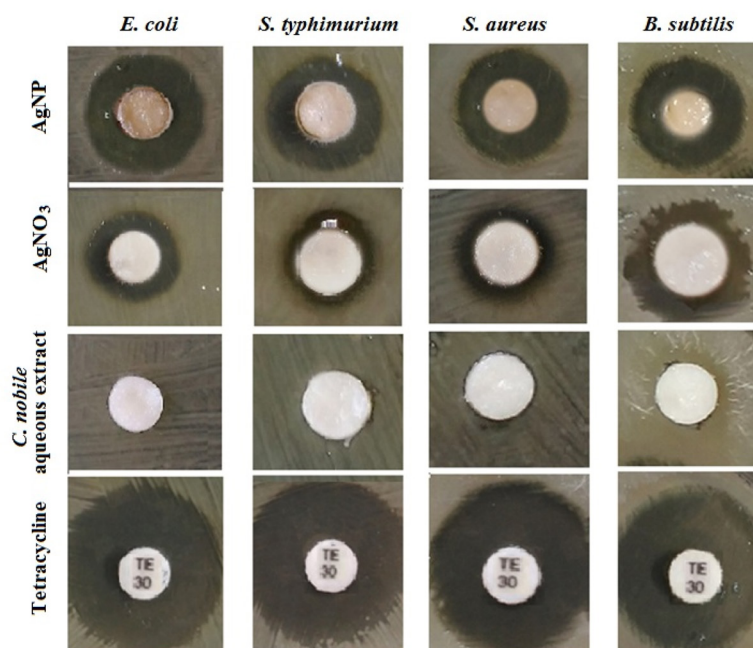


Figure 7. Antibacterial activity of synthesized Ag-NPs evaluated by disk diffusion method.

studies proposed the importance of hydrodynamic diameter for understanding and optimizing the size of nanoparticles and their performance in biological assays [41–44].

3.7 Antibacterial effect of silver nanoparticles

AgNPs have recently received a great deal of attention and concern due to their antibacterial activity [45]. In the present study, the biologically synthesized AgNPs showed an excellent antimicrobial activity against test microorganisms. Table 2 shows the result of antimicrobial activity for biosynthesized AgNPs, aqueous solution of AgNO₃ and aqueous extract of *C. nobile* and tetracycline by disk diffusion method. Clear zone around the disc was considered as the inhibitory effect. As it is shown in figure 7, AgNPs had respectable inhibition zone against all strains. The zone of inhibition of AgNPs for *E. coli*, *S. typhimurium*, *S. aureus* and *B. subtilis* was 15.1 ± 0.2, 14.3 ± 0.3, 13.0 ± 0.1 and 14.3 ± 0.2 mm, respectively. In general, AgNPs showed more anti-bactericidal activity compared with the AgNO₃ solution, the inhibition zone diameter

Table 2. Zone of inhibition (mm).

Bacteria	Zone of inhibition (mm) (mean ± SD of 3 replicates)			
	AgNPs	AgNO ₃	Tetracycline	<i>C. nobile</i>
<i>E. coli</i>	15.1 ± 0.2	8.1 ± 0.1	19.1 ± 0.2	NA ^a
<i>S. typhimurium</i>	14.3 ± 0.3	7.6 ± 0.4	19 ± 0.3	NA
<i>S. aureus</i>	13.0 ± 0.1	8.3 ± 0.2	18.3 ± 0.1	NA
<i>B. subtilis</i>	14.3 ± 0.2	8.0 ± 0.1	19.0 ± 0.2	NA

^a No antibacterial activity was found with the concentrations used in this work.

of AgNO₃ solution was 8.1 ± 0.1, 7.6 ± 0.4, 8.3 ± 0.2 and 8.0 ± 0.1 mm for *E. coli*, *S. typhimurium*, *S. aureus* and *B. subtilis*, respectively. It should be pointed out that the *C. nobile* extract showed no activity towards any of the organisms.

Moreover, the antimicrobial properties of synthesized silver nanoparticles were determined by means of minimal inhibition concentration (MIC) and minimal bactericidal concentration (MBC). MIC was recorded as the lowest concentration at

Table 3. Minimum inhibition concentrations (MIC) of AgNPs.

Bacteria	AgNPs		AgNO ₃		<i>C. nobile</i> aqueous extract	
	MIC (μg ml ⁻¹)	MBC (μg ml ⁻¹)	MIC (μg ml ⁻¹)	MBC (μg ml ⁻¹)	MIC (μg ml ⁻¹)	MBC (μg ml ⁻¹)
<i>E. coli</i>	7.8	15.6	15.6	15.6	NA ^a	NA
<i>S. typhimurium</i>	7.8	15.6	15.6	31.2	NA	NA
<i>S. aureus</i>	31.2	62.5	62.5	125	NA	NA
<i>B. subtilis</i>	15.6	31.2	31.2	62.5	NA	NA

^a No antibacterial activity was found with the concentrations used in this work.

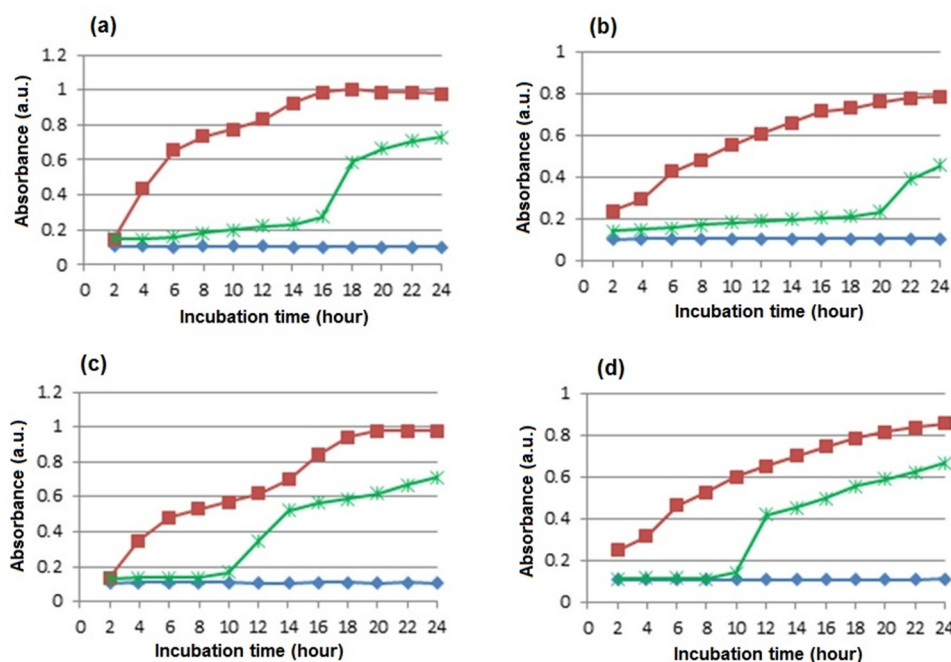


Figure 8. Growth curves of different bacterial strains exposed to Ag-NPs synthesized by *C. nobile* extract during 24 h: (a) *E. coli*, (b) *S. typhimurium*, (c) *S. aureus*, (d) *B. subtilis*. * (green star symbol): AgNPs with concentration of (a) 7.8 μg ml⁻¹ for *E. coli*, (b) 7.8 μg ml⁻¹ for *S. typhimurium*, (c) 31.2 μg ml⁻¹ for *S. aureus* and (d) 15.6 μg ml⁻¹ for *B. subtilis*. ♦ (blue diamond symbol): negative control, ■ (red square symbol): positive control.

which no visible growth of the test pathogens was observed. MIC values of the AgNPs against test microorganisms are presented in table 3. As it is shown in table 3, 7.8 μg ml⁻¹ proved to be MIC for *E. coli* and *S. typhimurium* while for *S. aureus* and *B. subtilis* MIC was recorded 31.2 μg ml⁻¹ and 15.6 μg ml⁻¹, respectively. In addition, for AgNO₃ the MICs values for *E. coli*, *S. typhimurium*, *S. aureus* and *B. subtilis* were found to be 15.6 μg ml⁻¹, 15.6 μg ml⁻¹, 62.5 μg ml⁻¹ and 31.2 μg ml⁻¹, respectively. Growth curves of different bacteria during the incubation period in the presence of various concentrations of AgNPs and AgNO₃ are presented in figures 8 and 9; absorbance spectra were measured by wavelength of 600 nm.

Table 3 shows the MBC values for AgNPs and AgNO₃, MBC is defined as the lowest concentration of the agent required to kill a particular bacterium. The MBC of AgNPs was 15.6 μg ml⁻¹ for *E. coli*, 15.6 μg ml⁻¹ for *S. typhimurium*, 62.5 μg ml⁻¹ for *S. aureus* and 31.2 μg ml⁻¹ for *B. subtilis*. In the case of AgNO₃ for gram negative bacteria *E. coli* and *S. typhimurium* the MBC was determined 15.6 μg ml⁻¹ and 31.2 μg ml⁻¹ while for gram positive bacteria *S. aureus* the MBC was 125 μg ml⁻¹ and for the *B. subtilis* the value was

62.5 μg ml⁻¹. The least MIC and MBC value of AgNPs than AgNO₃ may be due to the smaller size of the nanoparticles [46].

In general, gram negative bacteria *E. coli* and *S. typhimurium* showed better antimicrobial activity when compared to gram positive bacteria *S. aureus* and *B. subtilis*. These results agree with those presented by researchers which have reported that gram positive bacteria are less susceptible to the antimicrobial activity of silver [47–50]. Grigor’eva et al [51] investigated the cell responses to AgNPs for *S. aureus* and *S. typhimurium*. In this study they reported that overall damage of *S. aureus* culture was somewhat lower than that of the culture of *S. typhimurium* incubated with AgNPs during the same time. Goswami et al [52] reported larger zone of inhibition and lower MBC and MIC values for *E. coli* in comparison with *B. subtilis*. In studies of Martinez-Castanon et al [53] the lower MIC values for *E. coli* were compared against *S. aureus*. Furthermore, Kim et al [49] researches showed that AgNPs inhibit *E. coli* at the low concentration, whereas the growth-inhibitory effects on *S. aureus* were mild. Evidently, these differences in gram

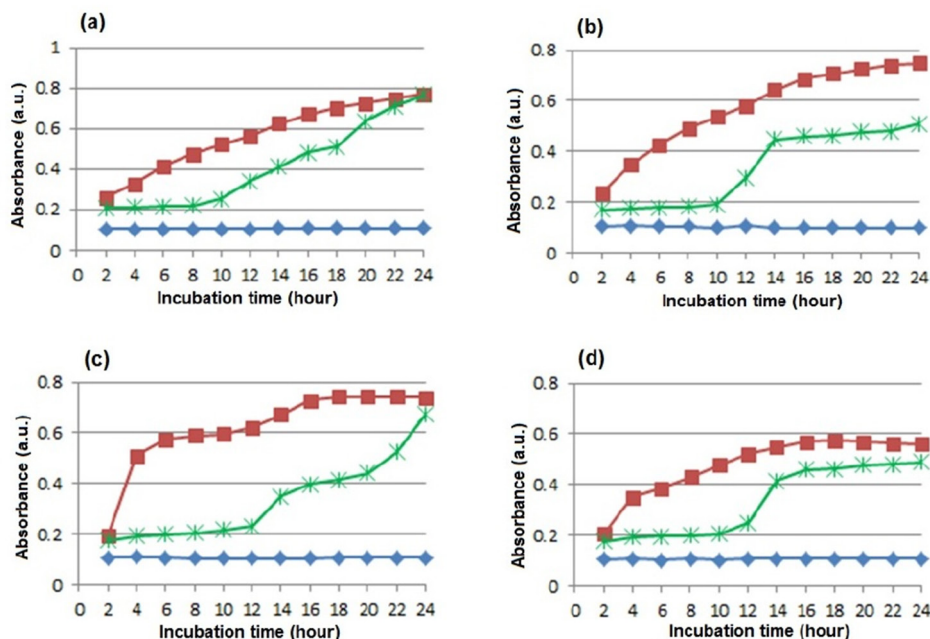


Figure 9. Growth curves of different bacterial strains exposed to AgNO_3 during 24 h: (a) *E. coli*, (b) *S. typhimurium*, (c) *S. aureus* and (d) *B. subtilis*. * (green star symbol): AgNO_3 with concentration of (a) $15.6 \mu\text{g ml}^{-1}$ for *E. coli*, (b) $15.6 \mu\text{g ml}^{-1}$ for *S. typhimurium*, (c) $62.5 \mu\text{g ml}^{-1}$ for *S. aureus* and (d) $31.2 \mu\text{g ml}^{-1}$ for *B. subtilis*. ♦ (blue diamond symbol): negative control, ■ (red square symbol): positive control.

positive and gram negative bacteria are based on structural features of cell envelope in these microorganisms [48, 51]. The cellular wall for gram positive strains is wider than the cellular wall for gram negative strains [54]. Thick cell wall of gram positive bacteria is because of their multiple layers of peptidoglycan compared to the cell wall of gram negative bacteria. Several layers of peptidoglycans and molecules of teichoic acids or lipoteichoic acids make a strong negative charge on the cell wall of gram positive bacteria which may contribute to sequestration of free silver ions. Therefore, the outer membrane of gram-positive bacteria may allow less silver to reach the cytoplasmic membrane than gram negative bacteria [47, 48, 55]. Consequently, gram negative bacteria are more susceptible.

4. Conclusion

Green synthesis is an ecofriendly and cost effective procedure for large scale production of nanoparticles. In the present study, silver nanoparticles were synthesized using *C. noble* aqueous extract. By changing the quantity of plant extract, silver ion concentration and reaction time at room temperature the size of nanoparticles was varied. At optimum condition the average diameter of AgNPs was 24 nm. The development of nanoparticles was monitored by UV-Vis spectroscopy and the primary particle size was measured by DLS. Characterization of nanoparticle at optimum condition was evaluated by TEM analysis and XRD measurements. FTIR analysis confirmed the bioreduction of Ag^+ ions to AgNPs by various functional groups. Moreover, the synthesized nanoparticles exhibit a pronounced antibacterial activity against different microorganisms.

Acknowledgments

The authors would like to thank the Research Council of Shiraz University and School of Veterinary Medicine, Shiraz University for financial and technical support of this study (Grant No. 71-GR-VT-5).

References

- [1] Jain D, Daima H K, Kachhwaha S and Kothari S 2009 *Dig. J. Nanomater. Bios.* **4** 557
- [2] Wang J and Wang Z 2007 *Mater. Lett.* **61** 4149
- [3] Yokoyama K and Welchons D 2007 *Nanotechnology* **18** 105101
- [4] Kohl Y et al 2011 *Nanomed. Nanotech. Biol. Med.* **7** 228
- [5] Meng H, Xue M, Zink J I and Nel A 2012 *J. Phys. Chem. Lett.* **3** 358
- [6] Gould I R, Lenhard J R, Muentner A A, Godleski S A and Farid S 2000 *J. Am. Chem. Soc.* **122** 11934
- [7] Wang Y and Toshima N 1997 *J. Phys. Chem. B* **101** 5301
- [8] Schmid G 1998 *Large metal clusters and colloids-metals in the embryonic state Structure, Dynamics and Properties of Disperse Colloidal Systems* vol 111, ed H Rehage and G Peschel (Germany: Springer) pp 52–57
- [9] Parak W J et al 2003 *Nanotechnology* **14** R15
- [10] Schultz D A 2003 *Curr. Opin. Biotechnol.* **14** 13
- [11] Nam J-M, Thaxton C S and Mirkin C A 2003 *Science* **301** 1884
- [12] Richardson A, Janiec A, Chan B and Crouch R 2006 *Chem. Educ.* **11** 331
- [13] Sharma V K, Yngard R A and Lin Y 2009 *Adv. Colloid Interface Sci.* **145** 83
- [14] Kumar V and Yadav S K 2009 *J. Chem. Technol. Biotechnol.* **84** 151
- [15] Edison T N J I, Lee Y R and Sethuraman M G 2016 *Spectrochim. Acta Mol. Biomol. Spectrosc.* **161** 122

- [16] Sre P R, Reka M, Poovazhagi R, Kumar M A and Murugesan K 2015 *Spectrochim. Acta Mol. Biomol. Spectrosc.* **135** 1137
- [17] Rajkuberan C, Sudha K, Sathishkumar G and Sivaramakrishnan S 2015 *Spectrochim. Acta Mol. Biomol. Spectrosc.* **136** 924
- [18] Sadeghi B, Rostami A and Momeni S 2015 *Spectrochim. Acta Mol. Biomol. Spectrosc.* **134** 326
- [19] Mariselvam R, Ranjitsingh A, Nanthini A U R, Kalirajan K, Padmalatha C and Selvakumar P M 2014 *Spectrochim. Acta Mol. Biomol. Spectrosc.* **129** 537
- [20] Kumar D A, Palanichamy V and Roopan S M 2014 *Spectrochim. Acta Mol. Biomol. Spectrosc.* **127** 168
- [21] Kathiravan V, Ravi S, Ashokkumar S, Velmurugan S, Elumalai K and Khatiwada C P 2015 *Spectrochim. Acta Mol. Biomol. Spectrosc.* **139** 200
- [22] Ashokkumar S, Ravi S, Kathiravan V and Velmurugan S 2014 *Spectrochim. Acta Mol. Biomol. Spectrosc.* **121** 88
- [23] Thirunavoukkarasu M, Balaji U, Behera S, Panda P and Mishra B 2013 *Spectrochim. Acta Mol. Biomol. Spectrosc.* **116** 424
- [24] Miri A, Sarani M, Bazaz M R and Darroudi M 2015 *Spectrochim. Acta Mol. Biomol. Spectrosc.* **141** 287
- [25] Raja K, Saravanakumar A and Vijayakumar R 2012 *Spectrochim. Acta Mol. Biomol. Spectrosc.* **97** 490
- [26] Nascimento G G, Locatelli J, Freitas P C and Silva G L 2000 *Braz. J. Microbiol.* **31** 247
- [27] Cho K-H, Park J-E, Osaka T and Park S-G 2005 *Electrochim. Acta* **51** 956
- [28] Li Z, Lee D, Sheng X, Cohen R E and Rubner M F 2006 *Langmuir* **22** 9820
- [29] PanáčĚk A et al 2006 *J. Phys. Chem. B* **110** 16248
- [30] Iravani S and Zolfaghari B 2013 *BioMed Res. Int.* **2013** 1
- [31] Ramar M et al 2015 *Spectrochim. Acta Mol. Biomol. Spectrosc.* **140** 223
- [32] Felice B, Prabhakaran M P, Rodríguez A P and Ramakrishna S 2014 *Mater. Sci. Eng. C* **41** 178
- [33] Zgoda J and Porter J 2001 *Pharm. Biol.* **39** 221
- [34] Nanda A and Saravanan M 2009 *Nanomed. Nanotech. Biol. Med.* **5** 452
- [35] Ibrahim H M 2015 *J. Radiat. Res. Appl. Sci.* **8** 265
- [36] Gavade N, Kadam A, Suwarnkar M, Ghodake V and Garadkar K 2015 *Spectrochim. Acta Mol. Biomol. Spectrosc.* **136** 953
- [37] Krishnaraj C, Ramachandran R, Mohan K and Kalaichelvan P 2012 *Spectrochim. Acta Mol. Biomol. Spectrosc.* **93** 95
- [38] Pourmortazavi S M, Taghdiri M, Makari V and Rahimi-Nasrabadi M 2015 *Spectrochim. Acta Mol. Biomol. Spectrosc.* **136** 1249
- [39] Ajitha B, Reddy Ya K and Reddy P S 2014 *Spectrochim. Acta Mol. Biomol. Spectrosc.* **128** 257
- [40] Philip D 2011 *Spectrochim. Acta Mol. Biomol. Spectrosc.* **78** 327
- [41] Cumberland S A and Lead J R 2009 *J. Chromatogr. A* **1216** 9099
- [42] Huang J et al 2007 *Nanotechnology* **18** 105
- [43] Samberg M E, Oldenburg S J and Monteiro-Riviere N A 2010 *Environ. Health Perspect.* **118** 407
- [44] Singhal G, Bhavesh R, Kasariya K, Sharma A R and Singh R P 2011 *J. Nanopart. Res.* **13** 2981
- [45] Shrivastava S, Bera T, Roy A, Singh G, Ramachandrarao P and Dash D 2007 *Nanotechnology* **18** 225103
- [46] Morones J R et al 2005 *Nanotechnology* **16** 2346
- [47] Egger S, Lehmann R P, Height M J, Loessner M J and Schuppler M 2009 *Appl. Environ. Microbiol.* **75** 2973
- [48] Kawahara K, Tsuruda K, Morishita M and Uchida M 2000 *Dent. Mater. J.* **16** 452
- [49] Kim J S et al 2007 *Nanomed. Nanotech. Biol. Med.* **3** 95
- [50] Pal S, Tak Y K and Song J M 2007 *Appl. Environ. Microbiol.* **73** 1712
- [51] Grigor'eva A et al 2013 *Biomaterials* **26** 479
- [52] Goswami A M, Sarkar T S and Ghosh S 2013 *AMB Express* **3** 16
- [53] Martinez-Castanon G, Nino-Martinez N, Martinez-Gutierrez F, Martinez-Mendoza J and Ruiz F 2008 *J. Nanopart. Res.* **10** 1343
- [54] Thiel J et al 2007 *Small* **3** 799
- [55] Manikandan R et al 2015 *Spectrochim. Acta Mol. Biomol. Spectrosc.* **138** 120